

Interactive Uncertainty Allocation and Trade-off at Early-stage Aircraft Computational Design

Arturo Molina-Cristóbal^{*}, Xin Chen[†], Marin D. Guenov[‡], Atif Riaz^{*} and Albert S.J. van Heerden[†]
School of Aerospace, Transport, and Manufacturing
Cranfield University, Cranfield, Bedfordshire, MK43 0AL, United Kingdom

A common probabilistic approach to uncertainty allocation is to assign acceptable variability in the sources of uncertainty, such that pre-specified probabilities of meeting performance constraints are satisfied. However, the computational cost of obtaining the associated trade-offs increases significantly when more sources of uncertainty and more outputs are considered. Consequently, visualizing and exploring the trade-off space becomes increasingly difficult, which, in turn, makes the decision-making process cumbersome for practicing designers. To tackle this problem, proposed is a parameterization of the input probability distribution functions, to account for several statistical moments. This, combined with efficient uncertainty propagation and inverse computation techniques, results in a computational system which performs order(s) of magnitude faster, compared with a combination of Monte Carlo Simulation and optimization techniques. Also, to aid decision-making regarding the potential combinations of uncertainty allocation, enablers for visualizing the trade space are proposed. The combined approach is demonstrated by means of a representative aircraft thermal system integration example.

Nomenclature

Y	=	Vector of outputs of interest
X	=	Vector of inputs of interest
h	=	Computational workflow, or model
f_x	=	Marginal probability density function
g_j	=	Constrain function of j^{th} output of interest
P_{g_j}	=	Pre-defined probabilities of satisfying j^{th} constraint
μ_x	=	Mean, first statistical moment
σ_x	=	Standard deviation, second statistical moment
γ_x	=	Skewness, third statistical moment
Γ_x	=	Kurtosis, fourth statistical moment
$Temp_{total}$	=	Total mean temperature, over all equipment surfaces
$Temp_{PC}$	=	Maximum surface temperature of the power center
$Temp_{BAT}$	=	Maximum surface temperature of the battery
\dot{m}_{PC}	=	Air mass flow extracted from power center
$Temp_{Fus}$	=	Fuselage reference temperature
$Temp_{NLG}$	=	Noise landing gear (NLG) reference temperature
HTC	=	Factor of fuselage, NLG, cargo wall, floor heat transfer coefficient
$Heat_{diss}$	=	Avionics equipment heat dissipation

^{*} Research Fellow, Centre for Aeronautics, Cranfield, MK43 0AL, United Kingdom.

[†] Research Student, Centre for Aeronautics, Cranfield, MK43 0AL, United Kingdom, AIAA Student Member.

[‡] Professor, Head of the Centre for Aeronautics, Cranfield, MK43 0AL, United Kingdom, AIAA Senior Member.

I. Introduction

THERE is currently a significant increase in efforts to incorporate Uncertainty Quantification and Management (UQ&M) techniques at the early design stages of complex engineering systems. In order to make well-informed decisions early in the design stage, when the maturity of design models is low and there is scant information on requirements, it is desirable to not only assess the impact of uncertainty, but also to reduce the uncertainty due to a lack of knowledge^{1,2}. As the iterative design loop progresses, more knowledge becomes available and uncertainty is reduced. This is done by, for example, directing resources to conduct preliminary analyses, with the objective of establishing the feasibility of a design^{3,4}. The decision of where to direct efforts to reduce uncertainty will be made based on the available information at hand and ‘engineering judgment’. A formal approach is to quantify and assign acceptable variability in the sources of uncertainty, such that a specified probability to meet a performance constraint is satisfied. In this paper, this approach is referred to as ‘uncertainty allocation’.

Allocating uncertainty is necessary to allow systems architects or designers to avoid situations where unknown variations in parameters or behaviors could lead to undesirable deviations in performance. In this way, risk is reduced. Uncertainty allocation is also useful for identifying different potential means of ensuring a desired probability of constraint satisfaction. Our research, as part of recent and current industry led projects, including TOICA^{5,6} and APROCONE⁷, indicates that uncertainty allocation is indeed considered as part of the decision-making process. However, it is based predominantly on experience, rather than on a systematic and formal framework. The result is that the decision-maker often may not be aware of the full set of options available and therefore which source(s) of uncertainty to trade.

Current UQ&M practices, such as robust design, optimization, and reliability analysis, involve minimizing or maximizing the outputs of interest (e.g., performance of the system), by systematically searching for design solutions that are robust against aleatory uncertainty and some classes of epistemic uncertainty (e.g., model uncertainty). While, these approaches are effective at finding robust solutions, they are not suited to address the uncertainty allocation problem. Chen et al.⁸ reported that inverse uncertainty propagation methods are essential enablers to solve the uncertainty allocation problem. Although methods have been developed for inverse uncertainty propagation using the Bayesian approach⁹, these may lead to relatively high computational cost and are not well suited in guiding the designer to make informed decisions when solving the uncertainty allocation problem.

Recently, methodologies to allocate uncertainty have been proposed by Opgenoord and Willcox¹⁰, which build on Curran and Wilcox¹¹. They presented a methodology, comprised of a sensitivity-based method, surrogate modelling and a weighted-sum optimization approach, to identify and select candidate uncertainty sources on which the reduction of uncertainty should be focused. However, in their method, the uncertainty on the input variables are applied only in the form of uniform probability distribution functions (PDFs).

In this paper, we address these limitations by proposing a method for interactive uncertainty allocation, to enable the investigation of input-variability trade-off strategies. The approach builds on the ‘inverse uncertainty propagation’ method, introduced by Chen et al.⁸. This method operates by inversely propagating uncertainty (represented as standard deviations) from the output variables to the input variables. It cannot, however, deal with many-to-many reversals (i.e. multiple outputs with multiple inputs). The specific objective of the work was to tackle this limitation by considering: a) more types of probability distribution functions (not just uniform PDFs), and b) not relying solely on the standard deviations of the PDFs of the inputs and outputs of interest. This, combined with enablers for visualizing the trade space, is intended to make the trade-off process more interactive and support more informed decision-making regarding the potential combinations of uncertainty allocation.

The paper is organized as follows. The problem and background information are presented in Section II. The proposed method is introduced in Section III. A demonstrative application of the method, using a representative aircraft thermal system integration example is presented in Section IV. Finally, conclusions are drawn and future work is outlined in Section V.

II. Problem Statement and Background

The uncertainty allocation problem can be approached as a reduction of uncertainty due to ‘lack of knowledge’, using the probability approach. A formal definition of the problem is as follows: consider changing (re-shaping) the probability distribution, by means of manipulating the parameters, \mathbf{d}_x , of the input probability density function, f_x , such that the required probabilities of constraint satisfactions are met. Mathematically, this can be formulated as:

$$\begin{aligned}
&\text{For a computational workflow, or model, } \mathbf{Y} = \mathbf{h}(\mathbf{X}), \\
&\quad \text{Find } f_{x_i}(x_i, \mathbf{d}_{x_i, p_i}), \quad i = 1, \dots, I, \\
&\quad \text{such that } P(y_j = g_j(\mathbf{X}) \leq 0) \geq P_{g_j}, \quad j = 1, \dots, J,
\end{aligned} \tag{1}$$

where,

$\mathbf{Y} = (y_1, \dots, y_J) \in \mathbb{R}^J$ is the vector of random output variables, or outputs of interest.

$\mathbf{X} = (x_1, \dots, x_I) \in \mathbb{R}^I$ is the vector of random input variables.

$f_{x_i}(x_i, \mathbf{d}_{x_i, p_i})$ is the probability density function (PDF) of the i^{th} input random variable.

$\mathbf{d}_{x_i, p_i} = (d_{x_i, 1}, \dots, d_{x_i, p_i}) \in \mathbb{R}^{p_i}$ is the vector of shape parameters that describe the shape of the probability density function, $f(x_i, \mathbf{d}_{x_i, p_i})$.

P_{g_j} are the pre-defined probabilities of satisfying the j^{th} constraint, $g_j(\mathbf{X}) = y_j(\mathbf{X}) - y'_j$; and y'_j is the quantile representing the constraint value of the j^{th} output of interest.

The problem, in an engineering context, is illustrated in Figure 1. Suppose, after propagating uncertainty forward through a computational workflow or model, $\mathbf{h}(\mathbf{X})$, the designer realizes that the probability of meeting a constraint, $P(g_i(\mathbf{X}) \leq 0)$, of the output variable affected by uncertainty, y_{g_i} , is not satisfactory. One course of action is then to investigate whether uncertainty in the input could be reduced. To do this, it needs to be known where to inversely allocate uncertainty affecting the input variables, \mathbf{X} , for a pre-defined probability of constraint satisfaction, P_{g_j} . In such cases, the designer will need to investigate the trade space to determine on which input variables the uncertainty should be allocated and to explore acceptable combinations of reduction from different sources, while guaranteeing that the performance will meet the probability of constraint satisfaction.

In general, Eq. (1) does not have analytical solutions. Therefore, it is necessary to simplify these equations, by making assumptions about the probability density functions (PDFs) and by breaking down the problem into steps to obtain numerical solutions. The next subsection introduces concepts of UQ&M techniques and design exploration methods that will be used to specify the enablers of the uncertainty allocation method proposed in this paper.

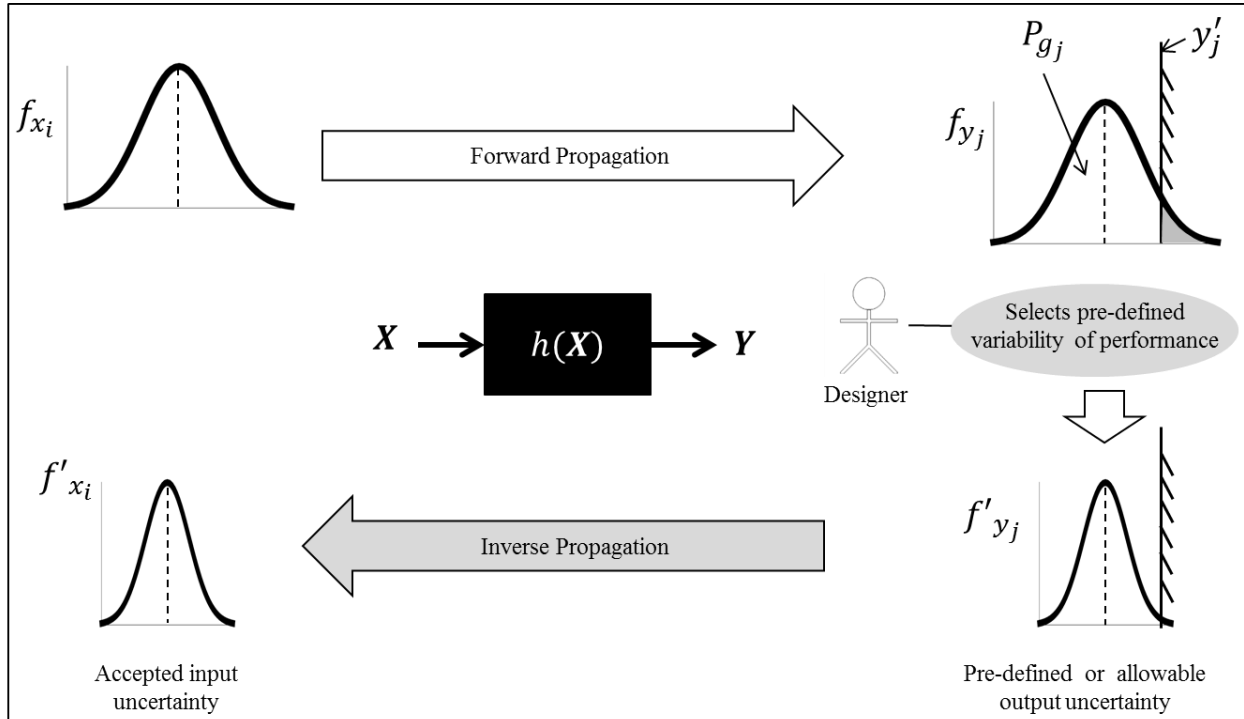


Figure 1. The process of allocating uncertainty.

A. UQ&M Techniques

The top part of the scenario illustrated in Figure 1 can be treated by existing UQ&M techniques. The purpose here would be to conduct a robustness analysis study to determine which outputs of interest do not meet the probability of constraint satisfaction. The existing methods comprise classical techniques to quantify and propagate sources of uncertainty through a computational model/workflow and also include robustness analyses.

There are different types of uncertainty and it has become common practice in engineering design and other fields to distinguish between two major classes – aleatory and epistemic uncertainty^{12,13}. Aleatory uncertainty is known as stochastic variability, or irreducible uncertainty, and exists because of the physical variability present in the system being analyzed, or in its environment (for example, atmospheric conditions). Epistemic uncertainty is known as reducible or subjective uncertainty and results from a lack of knowledge about the system. Both types of uncertainty will be present at the early stages of design, since there is usually a lack of data and the environmental conditions may not have been specified yet. In this paper, we consider only epistemic uncertainty and therefore assume that it can be reduced. Quantifying the sources of uncertainty in probabilistic terms requires elicitation at the outset, as discussed in O'Hagan and Oakley¹⁴. However, this is out of the scope of this paper and it will be assumed as given.

The next step is modelling of the elicited uncertainties as probability distributions. In turn, this requires that, the design problem has to be formulated as a computational process where the input and output variables of interest, workflow, objectives, and constraints must be specified.

The forward propagation, or ‘uncertainty propagation’, involves calculating the output distribution, or the statistical moments of the output. A fast propagation method, called Univariate Reduced Quadrature (URQ)¹⁵ can be used for this purpose, which requires the first four statistical moments of the uncertainty sources as input. This method is a generalization of the sigma-point method, which provides an estimate of the output mean and variance, and is able to handle asymmetric distributions. URQ requires significantly fewer evaluations than that needed for performing a Monte Carlo simulation, at comparable accuracy.

Robustness analysis takes place after the forward propagation of uncertainty is carried out. It is used to assess whether the design under uncertainty meets the requirements measured by the probability of constraint satisfaction on the outputs of interest.

B. Design Exploration Enablers

In order to visualize the trade space to identify potential solutions and make decisions regarding the allocation of uncertainty, an isocontour-based constraint analysis method and workflow reversal enablers are employed and described below.

1. Constraint analysis

This is a generalized isocontour-based constraint analysis method, developed by Riaz¹⁶. The method rapidly estimates the feasible region of the design space, using a DoE to compute discrete values of the constraint and then interpolating to find the curves corresponding to the constraints. For a design space with higher dimensions, slides of the design space can be plotted and exploration of the feasible region can be done by changing the ‘slice’ using the DoE levels points. This allows the decision-maker to gain insight into the topology of the feasible region(s) within the design space. This facilitates ‘what-if’ studies, where one is able to visualize the active constraints of a study and identify the potential design solutions, or explore the option of relaxing the constraints.

2. Workflow reversal

Reversal refers to the capability of ‘swapping’ the input and output variables of a computational workflow. In Chen et al.⁸, it was demonstrated that the standard deviation of an input variable of a default workflow (original sequencing) can be swapped with one of the standard deviations of the original output variables. This technique is based on a computational workflow management (CWM) method, developed by Balachandran et al.¹⁷ and Guenov et al.¹⁸, where the user is able to specify the variables he or she wants to swap, after which the reversed workflow is created. The CWM method enables the automatic formulation of the reversed workflow into an optimization problem and it is solved using a Gauss-Newton algorithm. This capability allows the investigation of ‘what-if’ scenarios and conducting flexible computational studies.

3. Interactive design exploration and visualization

It is argued here that the application of UQ&M techniques alone is not sufficient to handle the inherent uncertainty associated with early-stage design. An interactive and iterative learning process is necessary to address recognized design deficiencies and to refine the obtained solutions, as further design knowledge is acquired, for example, through the revision of design requirements and uncertainty allocation. To facilitate this interactivity, the

proposed methods have been implemented in a prototype software tool, called AirCADia¹⁸, which permits the designer to be actively involved in the decision-making process.

III. Proposed Method for Allocating Uncertainty and Trade-off Strategy

This section describes the method for allocating uncertainty and for setting up a trade-off strategy. The problem described in Eq. (1) is solved by considering multiple possible reductions of uncertainty, by means of exploring the shapes of the parametrized distributions functions. It is intended that the method enables swift assessment of the allocation of uncertainty, interactive trading-off of uncertainty from different contributing sources, and handling predefined uncertainty associated with performance and constraints. The method consists of five enablers:

A. Identification of Major Contributors

The aim of this step is to identify the major contributing sources of input uncertainty that impact the output variables of interest. Applying a global sensitivity analysis (using, for example, Sobol Indices and the Fourier Amplitude Sensitivity Test (FAST))¹⁹ can aid the designer to decide on which input variables efforts for reducing uncertainty should be focused. Once the major contributing sources of input uncertainty have been identified, their probability distribution functions can be parameterized, as described next.

B. Parametrization of the Input Probability Density Functions

One approach to find a suitable set of solutions that solve the problem described in Eq.(1), is to manipulate the statistical moments of the input PDFs, $f_{x_i}(x_i, d_{x_i, p_i})$, until all the probability of constraints satisfaction are met. In other words, the standard deviation could be reduced and/or the mean could be shifted and the same for the other moments, such as the skewness and kurtosis. Formulating the problem of finding multiple possible reductions of uncertainty, by directly manipulating the statistical moments of all input PDFs, poses the problem of guaranteeing that the input PDFs are realizable (not all combinations of moments can represent a PDF). To address this, we propose parametrizing the function that defines the shape of the PDFs, by linking the first fourth moments of a particular PDF with a single parameter, $d_{x,p}$. The parametrization must consider the fundamental properties of a PDF. The first property is that the density function be nonnegative ($0 < f_{x_i}(x_i, d_{x_i, p_i})$) for all x , whereas the second property is that a PDF has to have an area of unity (i.e. $\int f_{x_i}(x_i, d_{x_i, p_i}) dx = 1$).

However, when standard PDFs (e.g. Gaussian, Rayleigh, etc.) are parametrized, the parameters might not be suitable for uncertainty reduction or be definable in terms of ‘engineering’ quantities. Here, the parametrization aims at manipulating the shape of the PDF with variables that design practitioners are familiar with, such as the lower and upper bounds that define the range of variation (x_{lb_i} and x_{ub_i}). Also, the variations are often described as a percentage of the nominal value, x_{n_i} . Here, we specifically introduce a parametrization for two types of PDF, namely triangular and Gaussian mixture. However, this parameterization is not limited to these two. The shape parametrization is described below.

1. Parametrization for triangular distributions

The triangular PDF $f_t(x)$ is defined with the bounds x_{lb} and x_{ub} , on the x axis and the mode at x_n , as shown in Figure 2a. The parametrization is defined using the width ($d_x = x_{ub} - x_{lb}$) of the distribution. The PDF can then be re-shaped by scaling the width with respect to the nominal value, x_n . For a new width, d'_x , the new parameters of the PDF are calculated with geometrical proportions. Since the original and re-shaped triangular PDFs are proportional to each other (i.e., the lengths of the corresponding sides are proportional due to the unity area property of the triangle), the corresponding widths and the distance between x_n and the new bounds have lengths of the same ratio, as follows:

$$\begin{aligned} \frac{d'_x}{d_x} &= \frac{(x_n - x'_{lb})}{(x_n - x_{lb})}; \\ \frac{d'_x}{d_x} &= \frac{(x_n - x'_{ub})}{(x_n - x_{ub})}. \end{aligned} \quad (2)$$

The new bounds x'_{lb} and x'_{ub} can therefore be obtained from Eq. (2). After the new shape of the PDFs is defined, its first four moments are calculated and used for uncertainty propagation, (using for example URQ). For instance, the new mean and new variance of a triangular distribution are given by

$$\begin{aligned}
\mu'_x &= \frac{(x_n + x'_{ub} + x'_{lb})}{3}; \\
var'_x &= \frac{(x'_{ub} - x'_{lb})^2}{18} \left(1 - \frac{(x_n - x'_{lb})(x'_{ub} - x_n)}{(x'_{ub} - x'_{lb})^2} \right); \\
\gamma'_x &= \frac{\sqrt{2}(x'_{lb} + x'_{ub} - 2x_n)(2x'_{lb} - x'_{ub} - x_n)(x'_{lb} - 2x'_{ub} + x_n)}{5((x'_{lb})^2 + (x'_{ub})^2 + x_n^2 - x'_{lb}x'_{ub} - x'_{lb}x_n - x'_{ub}x_n)^{3/2}}.
\end{aligned} \tag{3}$$

The excess kurtosis, $\Gamma_x = -\frac{3}{5}$, remains invariant for a triangular PDF. Parametrization of uncertainty reduction can also be achieved by simply modifying either x_{ub} or/and x_{lb} with respect to x_n , thereby reducing the width.

2. Parametrization for Gaussian mixture distributions

In Figure 2b, the Gaussian mixture probability distribution²⁰, f_{gm} , is defined by two component functions with variances σ_1^2 and σ_2^2 and means μ_1 and μ_2 , with proportions α_1 and $\alpha_2 = 1 - \alpha_1$, so that

$$f_{gm}(x) = \alpha_1 \phi(x; \mu_1, \sigma_1^2) + \alpha_2 \phi(x; \mu_2, \sigma_2^2), \tag{4}$$

where $\phi(x; \mu, \sigma^2)$ denotes the univariate Gaussian PDF. The range of variability can be fitted by truncating ϕ at 3σ . The means can then be defined as: $\mu_1 = x_{lb} + 3\sigma_1$ and $\mu_2 = x_{ub} - 3\sigma_2$ (assuming $\mu_1 < \mu_2$); the standard deviations by $\sigma_1 = \sigma_2 = \frac{x_{ub} - x_{lb}}{8}$; the proportions by $\alpha_1 = \frac{|\mu_{x_l} - \mu_2|}{\mu_2 - \mu_1}$; whereas the nominal value, x_n , coincides with the mean μ_{x_l} of the Gaussian mixture PDF. Other Gaussian mixture parametric models can be found in McLachlan and Peel²⁰.

It is suggested that the Gaussian mixture PDF be parametrized in such a way that the skewness of the PDF can be manipulated by changing the position of the mean, μ_{x_l} . For example, it might be desirable to change the shape of f_{gm} from left-skewed (with mean μ_{x_l}) to right-skewed (with mean μ_{x_r}), as shown in Figure 2b. This can be achieved by switching the proportions of f_{gm} the skewness changes from being left-skewed to right-skewed, where the respective means are given by

$$\begin{aligned}
\mu_{x_l} &= \alpha_1 \mu_1 + \alpha_2 \mu_2; \\
\mu_{x_r} &= \alpha_2 \mu_1 + \alpha_1 \mu_2.
\end{aligned} \tag{5}$$

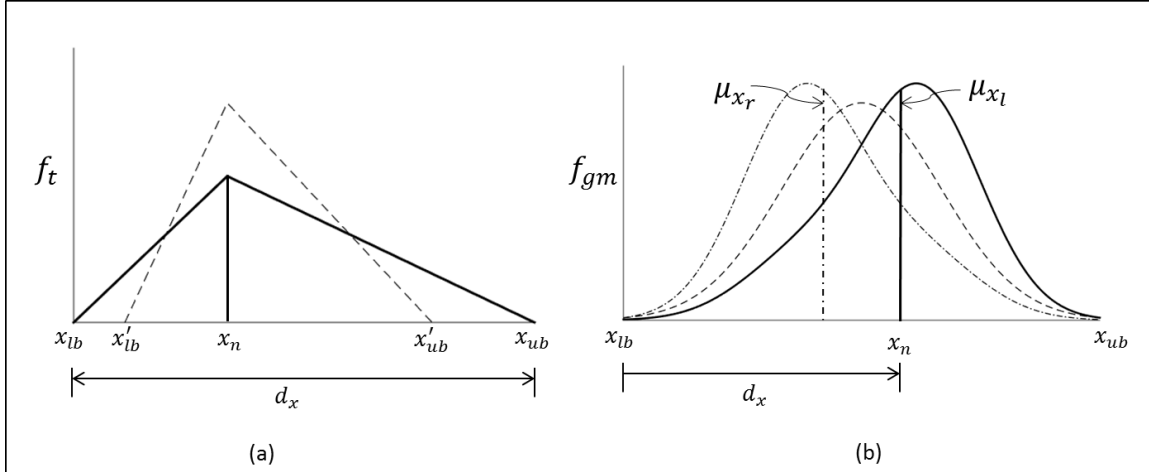


Figure 2. Parametrization of the input probability density function, a) triangular distribution and b) Gaussian mixture distribution.

For the shapes, in between the left- and right-skewed distributions (for example, a symmetric distribution), f_{gm} can be re-shaped by changing the nominal value, x_n (which is defined as $x_n = \mu'_x \in [\mu_{x_r}, \mu_{x_l}]$). The parametrization involves the linear transformation of component functions of Eq. (4) (i.e. new means, μ'_1 , μ'_2 , and new standard deviations, σ'_1 , σ'_2) by making changes to the position, $d'_x = \mu'_x$, as follows:

$$\begin{aligned}\mu'_1 &= \mu_1 + \Delta\mu; & \mu'_2 &= \mu_2 - \Delta\mu; \\ \sigma'_1 &= \frac{(\mu'_1 - x_{lb})}{3}; & \sigma'_2 &= \frac{(x_{ub} - \mu'_2)}{3},\end{aligned}\quad (6)$$

where $\Delta\mu$ is given by:

$$\Delta\mu = \begin{cases} (\mu_2 - \mu_1) \left(\frac{\mu_{x_l} - \mu'_x}{\mu_{x_l} - \mu_{x_r}} \right); & \alpha_1 = \frac{|\mu_{x_l} - \mu_2|}{\mu_2 - \mu_1}; \alpha_2 = 1 - \alpha_1; & \text{if } \mu'_x > \mu_{x_r} + \frac{(\mu_{x_l} - \mu_{x_r})}{2} \\ (\mu_2 - \mu_1) \left(\frac{\mu'_x - \mu_{x_r}}{\mu_{x_l} - \mu_{x_r}} \right); & \alpha_2 = \frac{|\mu_{x_l} - \mu_2|}{\mu_2 - \mu_1}; \alpha_1 = 1 - \alpha_2; & \text{otherwise.} \end{cases}\quad (7)$$

μ_{x_l} and μ_{x_r} are given in Eq. (5)

As mentioned before in the parametrization of the triangular PDF, after the new shape of the PDFs is defined, its first four moments are calculated and used for uncertainty propagation methods, such as URQ. Calculating the first four moments of a Gaussian mixture is well understood and can be found in McLachlan and Peel²⁰.

C. Composition of the Workflow for Uncertainty Allocation

The outer workflow is created in the following sequence:

- 1) An outer workflow is created to associate the first four moments (mean, μ_x , standard deviation, σ_x , skewness, γ_x , and kurtosis, Γ_x) of the input and the two moments of the output variables (mean, μ_y , and standard deviation, σ_y) as parameters (refer to the centre of Figure 3). This facilitates the application of rapid uncertainty propagation methods, such as URQ.
- 2) The parametrization of the PDFs (see the left of Figure 3) and the probability of constraint satisfactions (Figure 3, right) are linked to the outer workflow.

The result is a global workflow which links parameters d_{x_i, p_i} of the parametrized PDFs to the probability of constraint satisfactions of the outputs of interest and can be used for workflow reversal, which is indicated by the dotted arrows in Figure 3.

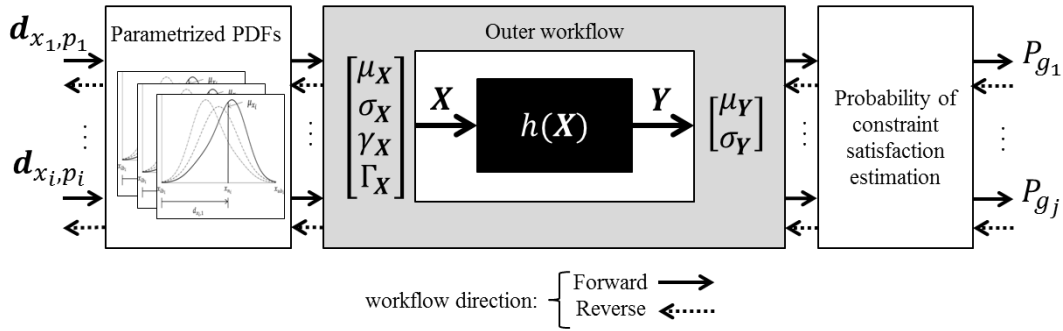


Figure 3. Outer workflow creation.

D. Visualization of the Trade-off Space

Often, the contributions from two (or more) sources of uncertainty in the input variables are comparable. In this case, the solution will have multiple combinations of reduced distributions. In other words, the solution of the uncertainty allocation problem is non-unique. In such a case, a Pareto front is sought.

The objective of this enabler is to visualize the multiple combinations as a trade-off space. This is done by computing the iso-contours corresponding to a particular value of the probability of constraint satisfaction. In this paper, the generalized isocontour-based constraint analysis method, described in Section IIB, is employed to do this. The curves are approximated by interpolating between the design of experiments (DoE) results. The set of the options of combinations to allocate the input uncertainty can be found along the ‘‘Pareto contour’’ (as represented by the black dots in Figure 4). This contour can be used to trade off these combinations of variabilities with each other. In practice, this may require the cost of reducing uncertainty to be considered. For example, in industrial scenarios, allocating resources to reduce uncertainty may imply the need for tighter manufacturing tolerances, which will increase the cost. Consideration of cost is important, but currently lies outside the scope of the current work. Rather the objective here is to change the value of the parameters or reduce the variability until the probability of constraint satisfaction is met. The possible combinations for uncertainty allocation along the resulting curve are analogous to

the Pareto solutions of a multi-objective optimization problem. The designer cannot minimize the reduction of the variability in one of the PDF parameters without further reducing the variability in the other PDF parameter. In the next section, the computation of the solutions is performed.

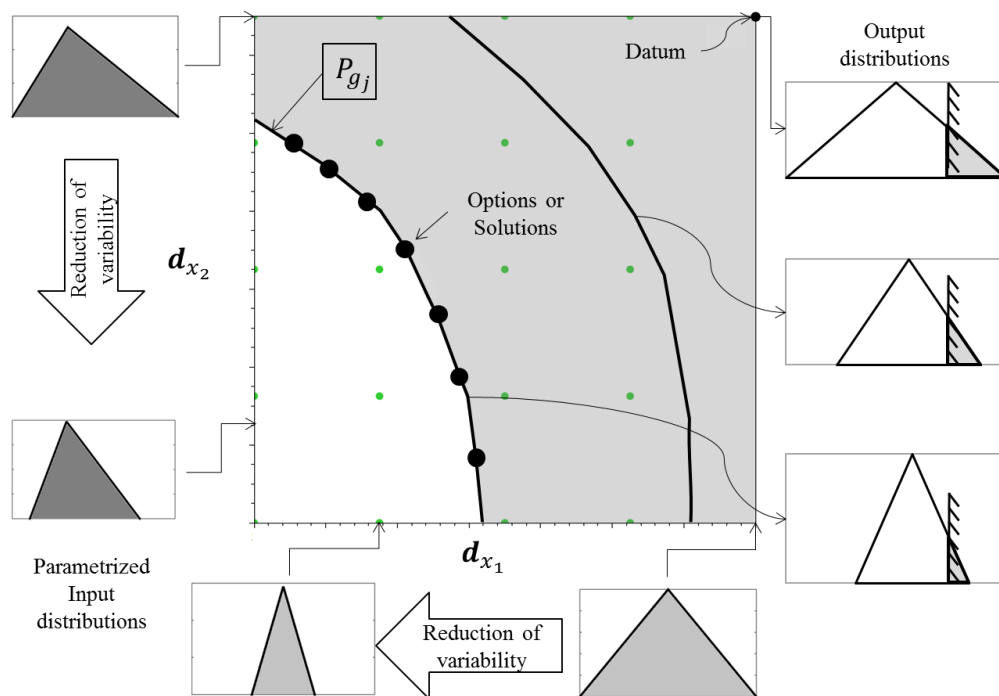


Figure 4. Trade-off space for allocating input distributions.

E. Uncertainty Allocation (Workflow Reversal)

The objective of this step is to generate a particular solution along the probability of constraint-satisfaction curve (black dots, in Figure 4, positioned along the P_{g_j} iso-contour). In other words, the workflow reversal is used to compute the pre-defined probability of constraint satisfaction as illustrated in Figure 1. This implies that this pre-defined probability must be considered (given) as an input, while in the default (forward) computational it is an output.

To do this, the CWM method (introduced in Section IIB2) for workflow reversal is employed. The workflow reversal allows one parameter from the input parameter vector, $\mathbf{d}_{x_i;p_i}$, to be swapped with one output from the set of probability constraints satisfaction, P_{g_j} .

When setting up the reversed workflow, the following procedure is proposed: in the case when reversing a single output with many inputs is required, the formulation of the reversal procedure will involve either constraining some of the inputs, to ensure that the number of unknown inputs and outputs are the same, or trading-off among the variability of the input variables.

The interactive visualization of 2D slices of the design space has been prototyped in the ‘AirCADia Explorer’ software¹⁸. This tool offers a powerful means for exploring the design space. Figure 5 shows the interface of AirCADia Explorer, where the user can interactively establish trade-off strategies to allocate uncertainty.

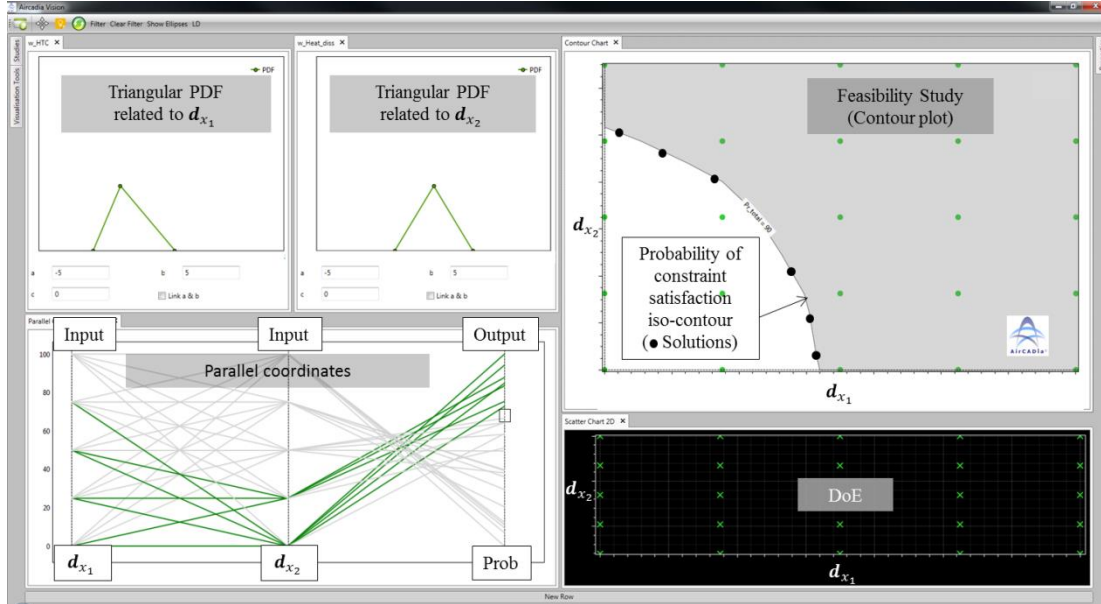


Figure 5. AirCADia Explorer prototype of the interactive margin and uncertainty allocation approach.

IV. An Industrial Example: Aircraft Thermal Integration Design

To demonstrate the methods, they were applied to a representative industrial problem concerning the thermal integration of the avionics of a single-aisle aircraft⁵ (see Figure 6). It is assumed that the design variables are affected by epistemic uncertainty and that the impact of this uncertainty on the thermal performance of the equipment needs to be assessed. It was also assumed that the equipment and the architecture of the avionics ventilation system had already been selected.

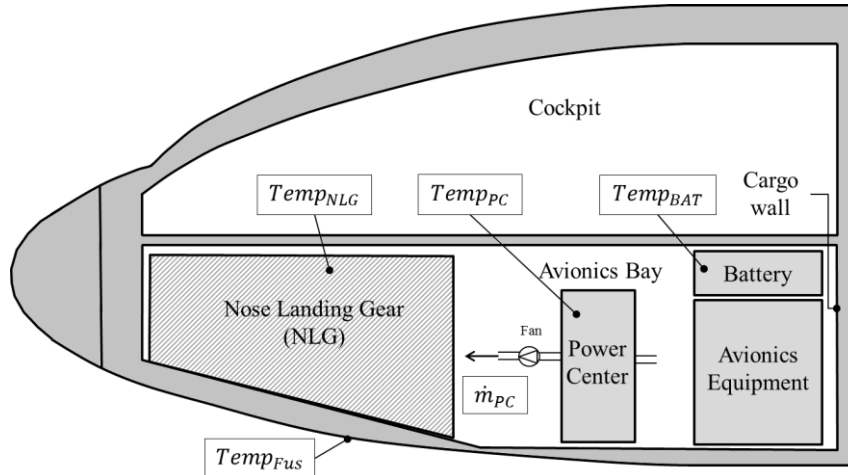


Figure 6. Illustration of the avionics equipment thermal integration design problem.

A. Problem Specification

The thermal performance of the avionics equipment was computed with a surrogate model of the Zonal Thermal Model (ZTM)²¹ which has five input variables and 69 output variables. For illustration purposes, we considered three outputs of interest, with the following respective thermal constraint (requirements):

- Total mean temperature, over all equipment surfaces: $Temp_{total} \leq 325.15 \text{ K } (52^\circ\text{C})$
- Maximum surface temperature of the power center: $Temp_{PC} \leq 319.15 \text{ K } (46^\circ\text{C})$
- Maximum surface temperature of the battery: $Temp_{BAT} \leq 324.15 \text{ K } (51^\circ\text{C})$

Uncertainty quantification was applied, under the following assumptions:

- It was assumed that each uncertainty input could be modelled in the form of an independent probability distribution function (e.g. a triangular or Gaussian mixture distribution, as was shown in Figure 2). The detailed specification for the problem is shown in Table 1.
- Variability in the inputs was considered to be the main source of uncertainty, whereas model uncertainty (simulation errors) was assumed to be negligible (in comparison with the sources of uncertainty listed in Table 1).

Table 1. Sources of uncertainty for the ZTM use case (data provided by Cappitelli and Mangeant²¹).

No.	Input variable	Nominal value and range of variability	Description of uncertainty	Probability distribution function
1	Air mass flow extracted from power center (\dot{m}_{PC})	0.0274 kg/s [0.0232, 0.0348]	Range of fluctuations	Rayleigh, $f_{\dot{m}_{PC}}$
2	Fuselage reference temperature ($Temp_{Fus}$)	$-8^{\circ}\text{C} \pm 5^{\circ}\text{C}$	Lack of definition (i.e. epistemic)	Gaussian, $f_{Temp_{Fus}}$
3	Factor of fuselage, NLG, cargo wall, floor heat transfer coefficient (HTC) [$\text{W}/\text{m}^2/\text{K}$]	1 -50%,+100%	Lack of definition (e.g. the material hasn't been selected yet)	Triangular, f_{HTC}
4	Avionics equipment heat dissipation ($Heat_{diss}$)	105 W/m^2 [85, 120]	Range of fluctuations of dissipated power	Normal Mixture, $f_{Heat_{diss}}$
5	NLG reference temperature ($Temp_{NLG}$)	$10^{\circ}\text{C} \pm 5^{\circ}\text{C}$	Lack of definition (i.e. epistemic)	Gaussian, $f_{Temp_{NLG}}$

The forward propagation was conducted by means of applying the URQ method (refer to the output section of Figure 7), which returns the mean and standard deviation of all output variables of interest. The numerical results are reported in Table 2. The designer can subsequently make assumptions regarding the shape of the distributions of the output variables, using the bounds on the probability of constraint satisfaction, or by comparing the results of uncertainty propagation with Monte Carlo Simulations (MCS). As can be seen in Figure 7, five thousand MCS points are enough to reach a confidence level of 95% on the estimate of the probability of constraint satisfaction. Also, it can be seen in Figure 7 that the MCS results can be approximated by Gaussian distributions. This is confirmed by plotting a Gaussian PDF in Figure 7 (output distributions), using the mean and standard deviation from the URQ forward propagation.

The result of this assessment confirmed that the probability of constraint satisfaction was not sufficient and it was required to be increased (to 95%). This problem could subsequently be formulated as an uncertainty allocation problem. The objective was therefore to find the parameters, \mathbf{d}_x , of the marginal probability distributions (see Table 1) that reduce the input uncertainty such that the probability to meet the thermal constraints of the avionics equipment is equal or greater to the requested probability of 95%. This can be stated mathematically as follows:

$$\begin{aligned}
 & \underset{\mathbf{d} \in \mathcal{A}}{\text{find}} (f'_{\dot{m}_{PC}}(\mathbf{d}_1), f'_{Temp_{Fus}}(\mathbf{d}_2), f'_{HTC}(\mathbf{d}_3), f'_{Heat_{diss}}(\mathbf{d}_4), f'_{Temp_{NLG}}(\mathbf{d}_5)) \\
 & \text{such that } \begin{cases} P(Temp_{total} \leq 325.15 \text{ K}) \geq 95\% \\ P(Temp_{PC} \leq 319.15 \text{ K}) \geq 95\% \\ P(Temp_{BAT} \leq 324.15 \text{ K}) \geq 95\% \end{cases} \quad (8)
 \end{aligned}$$

To this end, we have the scenario depicted Figure 1 and the proposed method can be applied, as described next.

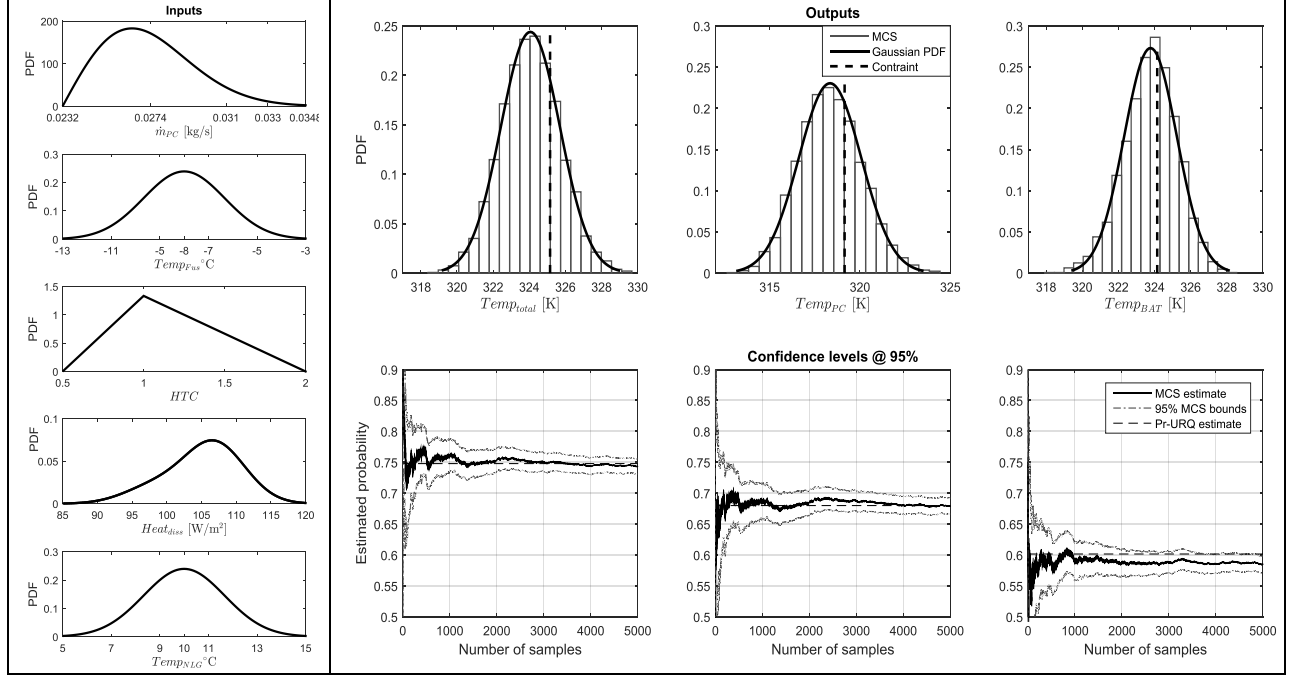


Figure 7. Forward propagation of uncertainty in the ZTM use case.

Table 2. Uncertainty propagation and robustness analysis results.

Output	Mean	Standard deviation	Constraint	Probability of constraint satisfaction
Total mean temperature over all equipment surfaces	324.0600 K	1.6379 K	$Temp_{total} \leq 325.15 \text{ K (} 52^\circ\text{C)}$	$P_{Temp_{total}}=74.78\%$
Maximum surface temperature of the power centre	318.3656 K	1.7358 K	$Temp_{PC} \leq 319.15 \text{ K (} 46^\circ\text{C)}$	$P_{Temp_{PC}}=67.99\%$
Maximum surface temperature of the battery	323.7787 K	1.4691 K	$Temp_{BAT} \leq 324.15 \text{ K (} 51^\circ\text{C)}$	$P_{Temp_{BAT}}=60.15\%$

B. Identification of Major Uncertainty Contributors for the ZTM Use Case

The aim of this enabler is to determine which sources of uncertainty have contributed the most to the variation in the output. A sensitivity analysis method, known as Fourier Amplitude Sensitivity Test (FAST)¹⁹ was employed. The results in Figure 8 show that, among all the inputs with uncertainty, two (HTC and $Heat_{diss}$) were the main contributors to the output uncertainty. In other words, the fluctuations (variability) of the heat dissipation of equipment, $Heat_{diss}$, and the lack of maturity of the data (variability) related to the heat transfer coefficient, HTC , of the materials contributed to the majority of uncertainty in the total-mean temperature over all equipment surfaces, $Temp_{total}$, the temperature of the power center, $Temp_{PC}$, and temperature of the battery, $Temp_{BAT}$. Therefore, it was decided that, to meet the probability of constraint satisfaction of the three outputs of interest, the variability on HTC and the variability on $Heat_{diss}$ had to be reduced. In addition, it was clear that the remaining input contributors were not influential enough on the outputs of interest and it was therefore deemed not necessary to conduct studies for the reduction of uncertainty in these. Subsequently, they remained fixed for the study.

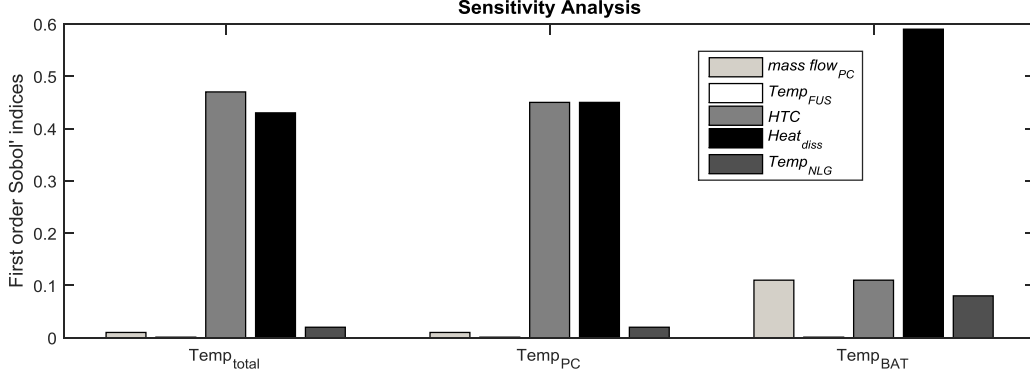


Figure 8. Sensitivity analysis results to identify contributions from different sources of uncertainty of the ZTM use case.

C. Uncertainty Parametrization of PDFs of the ZTM Use Case

The parametrization of the triangular distribution, f_{HTC} , and the Gaussian mixture PDFs, $f_{Heat_{diss}}$, was then performed, in the manner described in step two of section III. The shape of f_{HTC} was parametrized with respect to the base, or width, of the triangular distribution. Because high values of thermal material properties defined by HTC are desirable, only the variability on the left-hand side of the nominal value was reduced. The parameter used for uncertainty reduction was d_{HTC} . The shape of $f_{Heat_{diss}}$ was parameterized in two ways: first, the skewness was parametrized as illustrated in Figure 2b, where the parameter used for uncertainty reduction was $d_{Heat_{diss},\mu}$ of the Gaussian mixture PDF. The second way to reduce uncertainty was using the width, $d_{Heat_{diss},w}$, of the PDF, where the parametrization employed was the same as the triangular PDF illustrated in Figure 2a. A summary of the PDF parameter vector $\mathbf{d} = (d_{HTC}, d_{Heat_{diss},\mu}, d_{Heat_{diss},w})$ and its relation to the trade-off space is shown in Table 3.

Table 3. Specification of parameters of f_{HTC} and $f_{Heat_{diss}}$.

PDF & parameters relation	Parameter vector, $\mathbf{d} \in A$
$x'_{lb} = x_{ub} - d_{HTC}$	$d_{HTC} \in \{1, 1.125, 1.25, 1.375, 1.5\}$
$d_{Heat_{diss},\mu} = \mu'_x$	$d_{Heat_{diss},\mu} \in \{100, 101.25, 102.5, 103.75, 105\}$; [W/m ²]
$d_{Heat_{diss},w} = x_{ub} - x_{lb}$	$d_{Heat_{diss},w} \in \{5, 12.5, 20, 27.5, 35\}$; [W/m ²]

D. Creating the Workflow for the Thermal Integration Problem

An ‘outer workflow’ of the ZTM was created (as described in Section IIIC and depicted in Figure 3) to associate the statistical moments with the input and output variables of the model. These moments were further reformulated with parametrization of the f_{HTC} and $f_{Heat_{diss}}$ PDFs. The parametrization models, the outer workflow and the probability of constraint satisfaction model of the outputs of interest ($P_{Temp_{total}}$, $P_{Temp_{PC}}$, and $P_{Temp_{BAT}}$) constituted the entire workflow. Therefore, the user could specify the parametric variables d_{HTC} , $d_{Heat_{diss},1}$, and $d_{Heat_{diss},2}$ and then obtain the probability of output constraint satisfaction (indicated by the black arrows in Figure 3). Because there would subsequently be several combinations of the parametric variables that could potentially lead to 95% of probability, the next step was applied to visualize all these combinations.

E. Visualization of the Trade-off Space of the ZTM Use Case.

To explore multiple combinations of different distributions (uncertainty sources) using the workflow created in the previous step, the generalized isocontour-based constraint analysis method, described in Section IIB, was employed. The method starts by computing a DoE (full factorial sampling) of the design space, which, in this case, is specified by discretizing the PDF parameters into five levels each, as shown in Table 3.

The results can be presented as ‘slices’ of the 3D trade-off space, as depicted in Figure 9a-c. The three contours shown represent where the probability of constraint satisfaction surface intersects the slice. The ‘green dots’ are the samples of the DoE. The white area represents the feasible region, where the probability of satisfaction is higher than 95% for all the three outputs of interest, while the grey areas are infeasible. Note that the $P_{Temp_{PC}}$ and $P_{Temp_{BAT}}$ contours at 95% are active constraints and form a ‘Pareto front’. From Figure 9d, it can be seen that the

Pareto front resulting from this study is a surface of which slices (the cross section of the 3D design space through the point highlighted by the 'black dot') are shown in Figure 9a-c. The design space can be explored further by visualizing different combinations of slices, which can be obtained by 'moving' this intersection point. For example, the intersection point can be moved from the 'black dot' to the 'black triangle' (Figure 9) to create new slices.

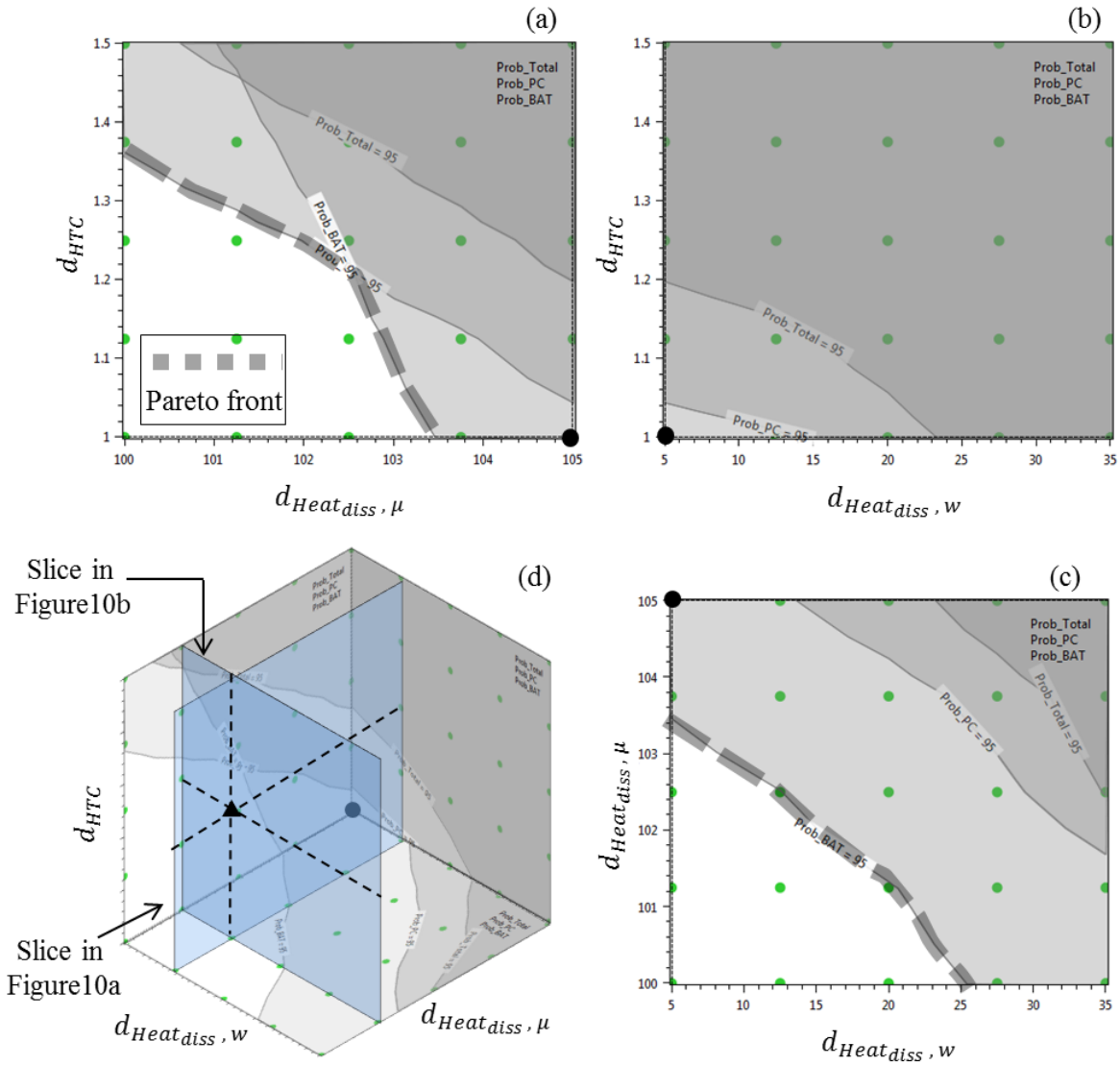


Figure 9. Slices of the trade-off space of the ZTM use case.

The purpose of such an exploration would be to find a region of the design space in which the Pareto front contains a combination of the parameters, \mathbf{d} , with a minimum reduction that meets the desired probability of constraint satisfaction. In the example shown, a satisfactory compromise regarding the reduction of all three parameters can be seen in Figure 10, where the slices are associated with an intersection point at $\mathbf{d} = (1.25, 101.5, 12.5)$ (represented by the black triangle in Figure 9d).

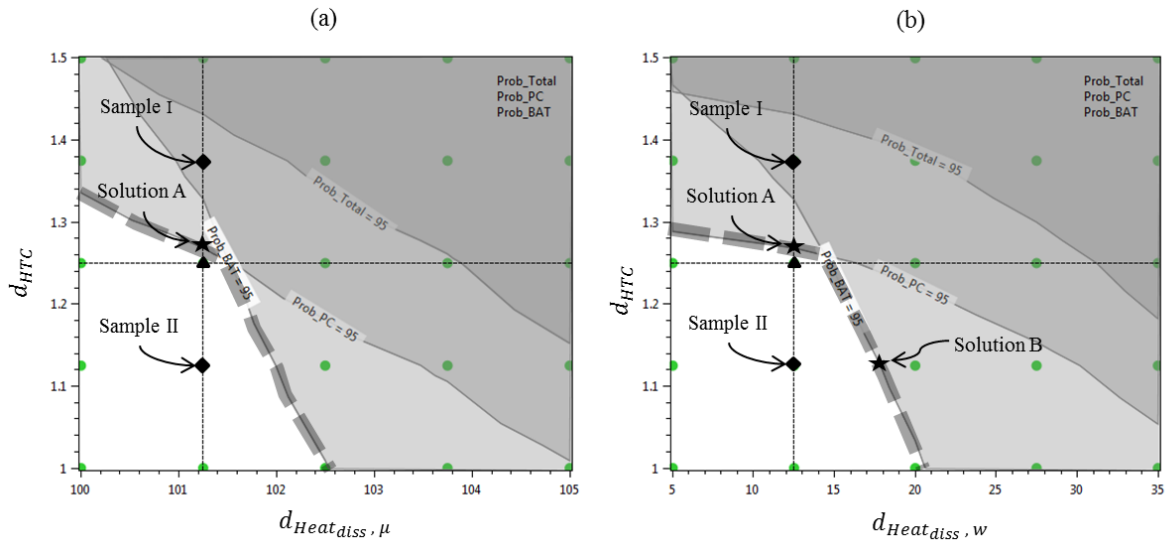


Figure 10. Trade-off space for uncertainty allocation.

Now, in the new slices of Figure 10, the user can explore possible options for allocating uncertainty to the two sources of uncertainty, by simply examining and choosing sample points from the DoE results. For example, Sample I in Figure 10 will not be chosen, since it is infeasible, i.e., only $P_{Temp_{total}}$ is satisfied, but not $P_{Temp_{PC}}$, or $P_{Temp_{BAT}}$. Sample II is a candidate, since it satisfies all constraints. However, regarding the 95% probability of constraint satisfaction, it may be reduced more than necessary. Recall that each simple point represents a new shape of the input PDFs. To illustrate this, the effects of choosing Sample I or II on the shapes of the parametrized input distributions can be seen in Figure 11. The ideal reduction will be along the ‘Pareto front’, for example solution ‘A’ (see Figure 10a-b), or ‘B’ (see Figure 10b). In the next section, it is described how the user can obtain such solutions by employing the workflow reversal method.

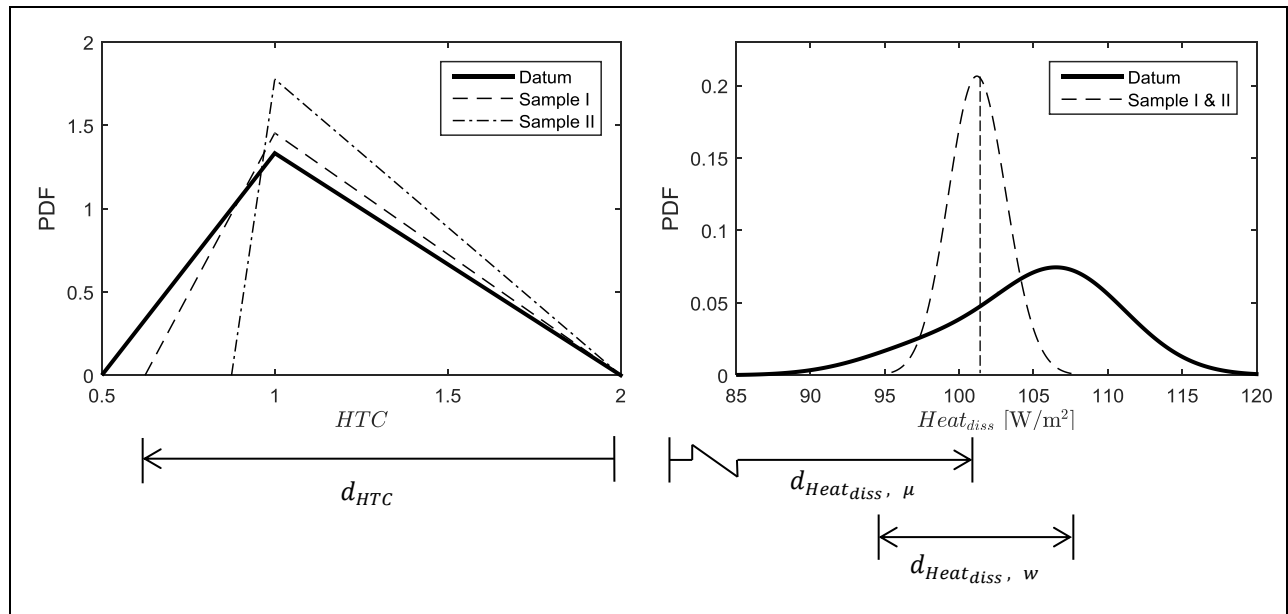


Figure 11. Parametrized input distributions.

F. Uncertainty Allocation (Workflow Reversal) for the ZTM Use Case

Employing the workflow reversal method described in Section IIB, the probability of output constraint satisfaction can be specified as a target. The execution of a reversed workflow could then compute how much uncertainty should be accepted from the inputs (i.e. the parametrized input PDFs) to achieve the target probability (indicated by the black dotted arrows in Figure 12). Here, two possible workflow reversal cases could be set up:

- 1) Reversal of the input variable related to the width, d_{HTC} , of the HTC PDF, with the output variable related to the probability of constraint satisfaction P_{TempPC} , while selecting the value of the parameters, $d_{Heat_{diss},\mu}$ and $d_{Heat_{diss},w}$, of the heat dissipation PDF (input). An example of the workflow reversal is depicted in Figure 12, while a sample solution in the trade-off space is marked as ‘Solution A’ in Figure 10.
- 2) Reversal of the input variable related to the skewness $d_{Heat_{diss},\mu}$ of the heat dissipation PDF, with the output variable related to the probability of constraint satisfaction of $P_{TempBAT}$, while selecting the value of the input parameters, $d_{Heat_{diss},w}$ and d_{HTC} . This example in the trade-off space is marked as ‘Solution B’ in Figure 10b.

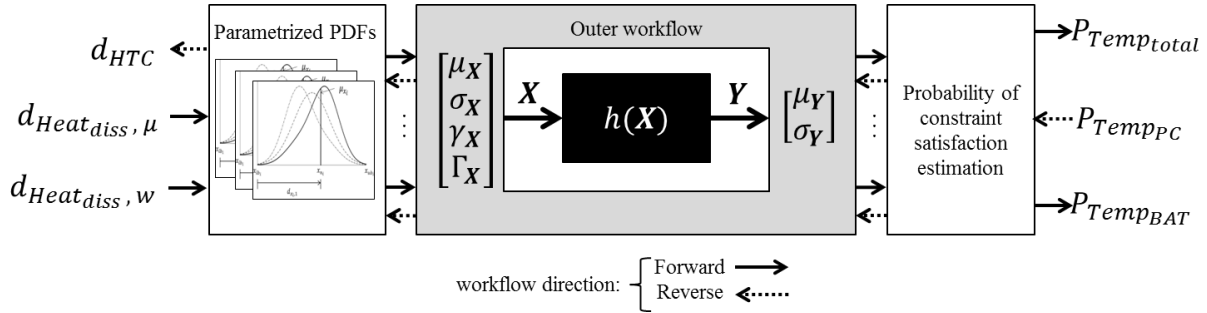


Figure 12. Example of a workflow reversal applied to the ZTM use case.

The designer needs to decide which trade-off strategy better suits the scenario. For this study, a trade-off scenario was assumed where it is known that the fluctuation of the heat dissipation of the equipment will not exceed $d_{Heat_{diss},w} = 12.5 \text{ W/m}^2$ and that the PDF could be skewed to the right with mean, $d_{Heat_{diss},\mu} = 101.2 \text{ W/m}^2$. In such a case, it is desired to determine how much variability, d_{HTC} , is acceptable in the value of the thermal property of the materials (heat transfer coefficient) in order to guarantee a 95% probability of satisfying the thermal constraint. To answer this, the designer may choose to set up the first workflow reversal case from the two possible cases discussed at the beginning of this subsection and depicted in Figure 12, in order to obtain the parameters of the PDFs for allocating uncertainty. This could be done with the interactive design environment, implemented in AirCADia Explorer (Figure 5), which formulates an optimization problem ‘on-the-fly’ and is solved using a Gauss-Newton algorithm. In Figure 13, the detailed descriptions of solutions A and B of the Pareto front is computed. Table 4 contains a summary of the results.

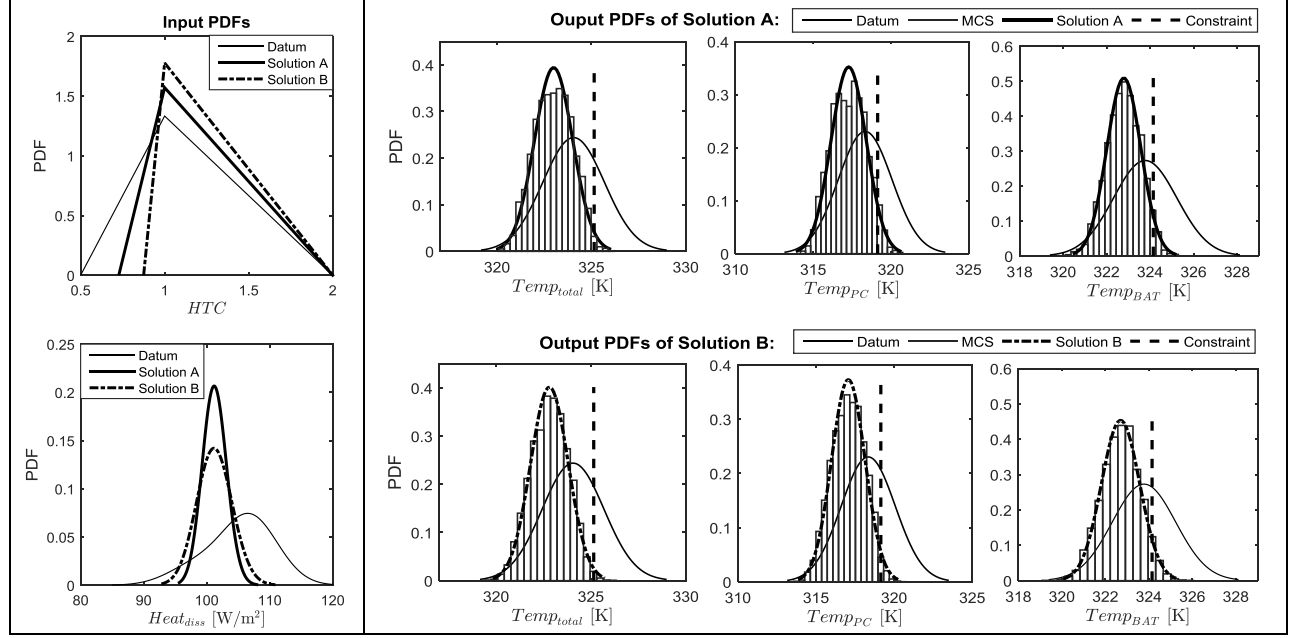


Figure 13. Results of uncertainty allocation in the ZTM use case.

Table 4. Comparison of input variability between before and after uncertainty allocation.

	Input variable HTC [$W/m^2/K$]		Input variable $Heat_{diss}$ [W/m^2]			Probability of constraint satisfaction via URQ & MCS *Pre-defined		
	Nominal value and range of variability	d_{HTC}	Nominal value and range of variability	$d_{Heat_{diss},w}$	$d_{Heat_{diss},\mu}$	$P_{Temp_{total}}$	$P_{Temp_{PC}}$	$P_{Temp_{BAT}}$
Datum	1 -50% /+100%	1.5	105 [85,102]	35	105	74.78%	67.99%	60.15%
Solution A	1 -27.3% /+100%	1.27	101.25 [95.44, 107.94]	12.5	101.25	98.309%	95%*	95.77%
Solution B	1 -12.5% /+100%	1.125	101.25 [92.812, 110.983]	18.169	101.25	99.065%	97.412%	95%*

G. Computational Efficiency

In this section, the efficiency of the proposed uncertainty allocation method is demonstrated by comparing it with an approach, devised by the authors, that combines optimization and MCS, as well as the methodology proposed by Opgenoord and Willcox^{10,22}. In the latter, the uncertainty allocation problem is formulated as a multi-objective optimization problem. Therefore, the problem stated in Eq.(8) needs to be reformulated as follows:

$$\begin{aligned}
 \min_{d \in \mathcal{A}} & \begin{cases} C_{HTC} = 1.5 - d_{HTC} \\ C_{Heat_{diss},\mu} = 105 - d_{Heat_{diss},\mu} \\ C_{Heat_{diss},w} = 35 - d_{Heat_{diss},w} \end{cases} \\
 \text{such that} & \begin{cases} P(Temp_{total} \leq 325.15 K) \geq 95\% \\ P(Temp_{PC} \leq 319.15 K) \geq 95\% \\ P(Temp_{BAT} \leq 324.15 K) \geq 95\% \end{cases} \quad (9)
 \end{aligned}$$

where A is the design space domain and C_{HTC} , $C_{Heat_{diss,\mu}}$ and $C_{Heat_{diss,w}}$ are the objective functions, defined as the ‘notional cost’ of reducing the uncertainty, as a function of the parameters of the HTC and $Heat_{diss}$ PDFs, respectively.

Shown in Table 5 is the comparison of the proposed uncertainty allocation method with the optimization approaches. It can be seen that solving the problem via the genetic algorithm could take up to 185 days on a desktop PC with an Intel Core i7-2600 @ 3.4 GHz processor, which is impractical.

In comparison, the CPU time used for the proposed uncertainty allocation method was approximately one hour and 33 minutes. Of course, alternative approaches can be taken to reduce computational time for the optimization approach, such as parallel computing, or employing alternative propagation methods. For example, the use of surrogates and Gauss-Legendre quadratures has been proposed by Opgenoord and Willcox¹⁰.

Although the Opgenoord and Willcox¹⁰ method only handles uniform PDFs on the input uncertainties and Eq.(8) has to be re-casted as weighted-sum optimization problem, the computational effort at each optimization iteration is estimated to be approximately 18 hours and 30 min. However, an important advantage of their approach is that they do not need to make the assumption that the output distributions are Gaussians.

Table 5. Computational cost comparison between the uncertainty allocation method and the optimisation approach.

Approach	Enablers/numerical treatments and required number of simulations ($n = 5$ input random variables)	Estimated CPU time (a single simulation of the ZTM ≈ 4 sec)
Proposed Uncertainty Allocation Method	DoE = $5*5*5=125$ URQ simulations ($2*n+1$) = 11 Gauss-Newton algorithm iterations = 2	$(125+2)*11=1397$ simulations require 93.13min of CPU time
Resource Allocation Optimization Formulation ¹⁰	Gauss-Legendre Quadrature, $(N_q)^n$ $N_q=7$ quadrature points in each dimension using the settings from Ref. 10	$7^5=16807$ simulations requires ≈ 18.5 hours of CPU time for a single optimization iteration
Uncertainty Allocation formulated as optimization problem in Eq.(5)	Employing a Multi-objective Genetic Algorithm: Typical Population ≈ 40 Moderate number of Generations ≈ 20 MCS = 5000	$40*20*5000 =$ 4000000 simulations require 185 days of CPU time

V. Summary and Conclusions

Presented in this paper is an efficient uncertainty allocation method which utilizes (shape) parametrization of the input probability distribution functions, allowing the manipulation of several statistical moments. The main advantages of the method include:

- The ability to vary all the first four statistical moments of the PDF allows more freedom for exploration, and ultimately for allocating input uncertainty. Moreover, the shape parametrization enables the the magnitude and spread of the uncertainty to be treated as decision variables, thereby allowing the exploration of the design space using ‘engineering’ quantities, rather than having to think in terms of statistical parameters.
- The ability to search for combinations of input uncertainties, or PDFs, that could reduce uncertainty on multiple outputs.
- The shape parameterization, combined with efficient uncertainty propagation and inverse computation techniques, results in a computational system which performs order(s) of magnitude faster, compared with a combination of Monte Carlo Simulation and optimization techniques.
- Finally, it is shown that, by visualizing the trade space of potential combinations of solutions to the uncertainty allocation problem, more informed decisions can be made when selecting an appropriate solution.

Future work will focus on: 1) addressing the limitation imposed by the requirement that the input probability distributions be independent; 2) removing the assumption that the output distributions are Gaussians, by calculating the other statistical moments; and 3) further development of visualization and interactive techniques, to deal with multi-dimensional trade spaces of the parameterized probability distribution functions.

Acknowledgments

The research leading to these results has received funding from the Aerospace Technology Institute (ATI) in the UK, under the Advanced Product Concept Analysis Environment (APROCONe) project (Ref no. 113092).

The authors gratefully thank Fabien Mangeant, Mario Cappitelli, and Michel Fouquembergh from Airbus Group Innovations for supplying the surrogate ZTM. We thank Sanjiv Sharma (Airbus-UK) for many insightful comments.

References

- ¹ de Rocquigny, E., Devictor, N., and Tarantola, S., *Uncertainty in industrial practice: a guide to quantitative uncertainty management*, John Wiley & Sons, 2008.
- ² Mangeant, F., “Joined initiatives around uncertainty management,” *Annals of telecommunications - annales des télécommunications*, vol. 66, p. 397. doi: 10.1007/s12243-011-0266-7
- ³ National Aeronautics and Space Administration, “NASA Systems Engineering Handbook, NASA/SP-2007-6105 Rev1,” *NASA/SP-2007-6105 Rev1*, 1995.
- ⁴ Thunnissen, D. P., and Tsuyuki, G. T., “Margin Determination in the Design and Development of a Thermal Control System,” *International Conference On Environmental Systems*, SAE International, 2004. doi: 10.4271/2004-01-2416
- ⁵ Arbez, P., “Innovations in Aircraft Architecture Trade-off,” *Seventh European Aeronautics Days: Aviation in Europe – Innovation for Growth*, London: 2015.
- ⁶ Rouvreau, S., Mangeant, F., and Arbez, P., “TOICA Innovations in Aircraft Architecture Selection, Uncertainty Management in Collaborative Trade-offs,” *6th IC-EpsMsO - 6th International Conference on Experiments/Process/System Modeling/Simulation/Optimization*, Athens, Greece: 2015.
- ⁷ Research Councils UK, “Advanced Product Concept Analysis Environment (APROCONe), Project Reference: 113092,” *RCUK gateway* Available: <http://gtr.rcuk.ac.uk/projects?ref=113092>.
- ⁸ Chen, X., Molina-Cristobal, A., Guenov, M. D., Datta, V. D., and Riaz, A., “A Novel Method for Inverse Uncertainty Propagation,” *11th International Conference on Evolutionary and Deterministic Methods for Design, Optimization and Control with Applications to Industrial and Societal Problems, EUROGEN-2015*, Glasgow, UK: 2015.
- ⁹ Litvinenko, A., and Matthies, H. G., “Inverse problems and uncertainty quantification,” *arXiv preprint arXiv:1312.5048*, 2013.
- ¹⁰ Opgenoord, M. M. J., and Willcox, K. E., “Sensitivity Analysis Methods for Uncertainty Budgeting in System Design,” *AIAA Journal*, vol. 54, 2016, pp. 3134–3148. doi: 10.2514/1.J054743
- ¹¹ Curran, Q. C., and Willcox, K. E., “Sensitivity Analysis Methods for Mitigating Uncertainty in Engineering System Design,” *56th AIAA/ASCE/AHS/ASC Structures, Structural Dynamics, and Materials Conference*, 2015, p. 899. doi: 10.2514/6.2015-0899
- ¹² Oberkampf, W., Helton, J., and Sentz, K., “Mathematical representation of uncertainty,” *19th AIAA Applied Aerodynamics Conference*, 2001, p. 1645. doi: 10.2514/6.2001-1645
- ¹³ Helton, J. C., “Uncertainty and sensitivity analysis in the presence of stochastic and subjective uncertainty,” *Journal of Statistical Computation and Simulation*, vol. 57, 1997, pp. 3–76. doi: 10.1080/00949659708811803
- ¹⁴ O’Hagan, A., and Oakley, J. E., “Probability is perfect, but we can’t elicit it perfectly,” *Reliability Engineering & System Safety*, vol. 85, 2004, pp. 239–248. doi: 10.1016/j.ress.2004.03.014
- ¹⁵ Padulo, M., Campobasso, M. S., and Guenov, M. D., “Novel Uncertainty Propagation Method for Robust Aerodynamic Design,” *AIAA Journal*, vol. 49, 2011, pp. 530–543. doi:10.2514/1.J050448
- ¹⁶ Riaz, A., “A Set-Based Approach to Passenger Aircraft Family Design,” PhD Thesis, Cranfield University, 2015.
- ¹⁷ Balachandran, L., Fantini, P., and Guenov, M., “Computational Process Management for Aircraft Conceptual Design,” *7th AIAA ATIO Conf, 2nd CEIAT Int’l Conf on Innov and Integr in Aero Sciences, 17th LTA Systems Tech Conf; followed by 2nd TEOS Forum*, American Institute of Aeronautics and Astronautics, 2007.
- ¹⁸ Guenov, M. D., Nunez, M., Molina-Cristóbal, A., Sripawadkul, V., Datta, V., and Riaz, A., “Composition, Management and Exploration of Computational Studies at Early Design Stage,” *Computational Intelligence in Aerospace Sciences*, M. Vasile and V. Becerra, eds., American Institute of Aeronautics and Astronautics, 2014. doi: 10.2514/5.9781624102714.0415.0460
- ¹⁹ Cukier, R. I., Fortuin, C. M., Shuler, K. E., Petschek, A. G., and Schaibly, J. H., “Study of the sensitivity of coupled reaction systems to uncertainties in rate coefficients. I Theory,” *The Journal of Chemical Physics*, vol. 59, 1973, pp. 3873–3878.
- ²⁰ McLachlan, G., and Peel, D., *Finite mixture models*, New York, USA: John Wiley & Sons, 2004. doi: 10.1063/1.1680571
- ²¹ Cappitelli, M., Mangeant, F., and Fouquembergh, M., “(TOICA Partners from Airbus Group Innovations), Personal Communication, 10 February 2016,” 2016.
- ²² Opgenoord, M. M. J., Allaire, D. L., and Willcox, K. E., “Variance-Based Sensitivity Analysis to Support Simulation-Based Design Under Uncertainty,” *Journal of Mechanical Design*, vol. 138, Sep. 2016, pp. 111410–111412. doi: 10.1115/1.4034224